

Superconducting Gap Structure of Filled Skutterudite $\text{LaOs}_4\text{As}_{12}$ Compound through μSR Investigations

A. Bhattacharyya,^{1,*} D. T. Adroja,^{2,3,†} A. D. Hillier,² and P. K. Biswas^{2,‡}

¹*Department of Physics, Ramakrishna Mission Vivekananda Educational and Research Institute, Belur Math, Howrah 711202, West Bengal, India*

²*ISIS Facility, Rutherford Appleton Laboratory, Chilton, Didcot Oxon, OX11 0QX, United Kingdom*

³*Highly Correlated Matter Research Group, Physics Department, University of Johannesburg, PO Box 524, Auckland Park 2006, South Africa*

(Dated: July 11, 2023)

Filled skutterudite compounds have gained attention recently as an innovative platforms for studying intriguing low-temperature superconducting properties. Regarding the symmetry of the superconducting gap, contradicting findings from several experiments have been made for $\text{LaRu}_4\text{As}_{12}$ and its isoelectronic counterpart, $\text{LaOs}_4\text{As}_{12}$. In this vein, we report comprehensive bulk and microscopic results on $\text{LaOs}_4\text{As}_{12}$ utilizing specific heat analysis and muon-spin rotation/relaxation (μSR) measurements. Bulk superconductivity with $T_C = 3.2$ K was confirmed by heat capacity. The superconducting ground state of the filled-skutterudite $\text{LaOs}_4\text{As}_{12}$ compound is found to have two key characteristics: superfluid density exhibits saturation type behavior at low temperature, which points to a fully gapped superconductivity with gap value of $2\Delta/k_B T_C = 3.26$; additionally, the superconducting state does not show any sign of spontaneous magnetic field, supporting the preservation of time-reversal symmetry. These results open the door for the development of La-based skutterudites as special probes for examining the interplay of single- and multiband superconductivity in classical electron-phonon systems.

I. INTRODUCTION

Due to their potential as thermoelectric materials for either refrigeration or power generation applications, many filled skutterudite compounds with RT_4X_{12} stoichiometry (R = alkali metals, alkaline earth metals, lanthanides, or light actinides; T = Fe, Os, Ru; X = P, As, Sb) have lately been the focus of several investigations [1–3]. With two formula units RT_4X_{12} per unit cell, these compounds form a body-centered cubic structure (space group $Im\bar{3}$, No: 204). The structures consist of rigid covalently bonded cage-forming frameworks T_4X_{12} that encapsulate various bonded guest atoms R. This leads to local anharmonic thermal vibrations (rattling modes), which would reduce phononic heat conduction and open the door to their potential as promising thermoelectric materials. Because of the significant hybridization between the $4f$ band manifold and electronic conduction states, as well as the degree of freedom provided by the R- f -derived multipole momenta of the cubically symmetric X_{12} cages, those compounds may include a variety of distinct electronic and magnetic ground states. For examples, consider unconventional superconductivity [4–8], Kondo effect [9–13], heavy fermions [14], non-Fermi liquid behavior [9], etc.

The majority of the Pr- and Ce-based filled skutterudite compounds are hybridized gap semiconductors or show magnetic transitions, however $\text{PrOs}_4\text{Sb}_{12}$ [4, 5], $\text{PrRu}_4\text{Sb}_{12}$ [6] and $\text{PrRu}_4\text{As}_{12}$ [15] show superconducting transitions at

1.8 K, 0.97 K and 2.4 K, respectively. $\text{PrOs}_4\text{Sb}_{12}$ is highly intriguing for a variety of reasons [16], including: (i) it is the first known example of a heavy-fermion superconductor containing Pr; (ii) it shows unconventional strong-coupling superconductivity that breaks time-reversal symmetry; and (iii) instead of magnetic fluctuations, electric quadrupole fluctuations may be involved in the superconducting pairing process. The unique band structure of these compounds and the hybridization effects between localized f electrons and conduction electrons appear to play a crucial role, in addition to the fact that the origin of the majority of those unconventional phenomenologies is unknown. It was recently revealed that the Fermi level of La compounds is placed at a prominent peak arising from the T- d band manifold, which might contribute to electronic instability [1, 17]. Several La-based compounds $\text{LaT}_4\text{X}_{12}$ are especially remarkable within the filled skutterudite class due to their remarkable superconducting properties. For examples, $\text{LaFe}_4\text{P}_{12}$ ($T_C = 4.1$ K) [18], $\text{LaOs}_4\text{P}_{12}$ ($T_C = 1.8$ K) [18, 19], and $\text{LaRu}_4\text{Sb}_{12}$ ($T_C = 3.6$ K) [9, 20], with a special attention to the $\text{LaRu}_4\text{As}_{12}$ ($T_C = 10.3$ K, $H_{c2} = 10.2$ T)- with the highest superconducting transition temperature. [15, 19, 21].

The ratio of the heat capacity jump ΔC to γT_C is $\Delta C/(\gamma T_C) = 1.75$ for $\text{LaRu}_4\text{As}_{12}$ comparison to the BCS value of 1.43 [15]. While the majority of La-based filled skutterudites are completely gapped superconductors, past research has shown numerous unique aspects of $\text{LaRu}_4\text{As}_{12}$, such as a positive curvature of H_{c2} , nonexponential behavior of the electronic heat capacity, and square root field dependency of the Sommerfeld coefficient (γ) [22]. We recently reported unambiguous evidence of multiband $s + s$ -wave superconductivity in $\text{LaRu}_4\text{As}_{12}$ using muon-spin rotation measurements, with $2\Delta_1/k_B T_C = 3.73$ for the larger gap and $2\Delta_2/k_B T_C = 0.144$ for the smaller gap [23]. Furthermore,

* amitava.bhattacharyya@rkmvu.ac.in

† devashibhai.adroja@stfc.ac.uk

‡ Deceased

inelastic X-ray scattering experiments indicated essentially temperature-independent phonon modes between 300 K and 20 K, with the exception of 2 K, where a weak softening of the specific phonon modes is detected [23]. All of these results demonstrate the relevance of the electron–phonon interaction in the superconductivity of $\text{LaRu}_4\text{As}_{12}$, and they accord well with the DFT-based phonon simulations [24].

Another isostructural La-based filled skutterudite compound, $\text{LaOs}_4\text{As}_{12}$, has been reported by Shirovani et al. to exhibit superconductivity with $T_C = 3.2$ K [21]. $\text{LaOs}_4\text{As}_{12}$ has also shown some signs of multiband superconductivity, such as the upward curving of the upper critical field around the transition temperature and unusual behavior in the electronic specific heat data [25]. A single-gap, s-wave superconducting ground state, however, is suggested by a recent study of the temperature dependency of lower critical field [26]. Another study found that the high-amplitude lanthanum phonons dominate the vibrational eigenmodes at low energies based on the phonon dispersion relation determined from inelastic neutron scattering experiments [27].

We have thus performed systematic muon-spin rotation and relaxation (μSR) measurements to examine the superconducting pairing process in the $\text{LaOs}_4\text{As}_{12}$ compound. Contrary to prior experimental work asserting two-band superconductivity [25], we demonstrate that the low-temperature behavior of the superfluid density points to a fully gapped superconducting Fermi surface. Furthermore, the preservation of time-reversal symmetry is confirmed by the lack of spontaneous magnetic fields in the superconducting state, ruling out unusual pairing processes. The transition from two-band to single-band superconductivity in $\text{LaRu}_4\text{As}_{12}$ to $\text{LaOs}_4\text{As}_{12}$ is caused by differences in interband coupling strength in the Fermi surface, as evidenced by the different degrees of hybridization and electronic properties observed in the Fermi surfaces of both compounds [28]. These results underline the significance of $\text{LaRu}_4\text{As}_{12}$ and $\text{LaOs}_4\text{As}_{12}$ compounds as an important platform for investigating filled skutterudites for the competition between single-band and multiband superconductivity in electron–phonon driven systems.

II. EXPERIMENTAL DETAILS

The high-temperature molten-metal-flux technique, described in [29], was used to grow single crystals of $\text{LaOs}_4\text{As}_{12}$. In a quartz ampule, elements with purities higher than 99.9% and a molar ratio of $\text{La}:\text{Os}:\text{Cd}:\text{As} \rightarrow 1:4:12:48$ were combined. The details on the single crystal growth can be found in [29]. The relaxation approach was used to measure the heat capacity in a Quantum Design physical properties measurement (PPMS) system. Temperatures as low as 0.38 K were attained utilizing a He-3 attachment to the PPMS [25].

The μSR measurements were carried out using small size

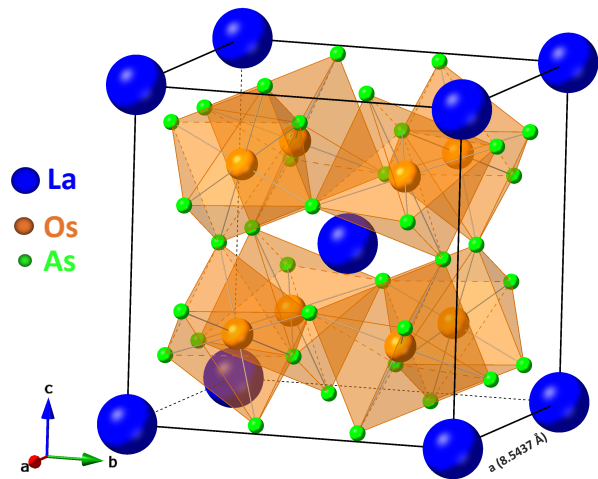


Figure 1. A unit cell of the body-centered cubic $\text{LaOs}_4\text{As}_{12}$ structure with the space group $Im\bar{3}$ that crystallizes within a CoAs_3 -type skutterudite structure packed with La atoms. Green: As, Orange: Os, and Blue: La.

unaligned single crystals ($0.1 \text{ mm} \times 0.1 \text{ mm} \times 0.1 \text{ mm}$, total mass 1 g), which gave powder average muon signal, of $\text{LaOs}_4\text{As}_{12}$. The μSR spectrometer at the Rutherford Appleton Laboratory, ISIS Neutron and Muon Source in the UK was used to perform the μSR measurements [30]. In a μSR experiment, the sample is injected with 100% spin-polarized muons. Each implanted muon thermalizes, at which point it decays (lifetime $\tau_\mu = 2.2 \mu\text{s}$) into a positron (and two neutrinos) which is preferentially released in the direction of the muon spin at the moment of decay. Utilizing detectors carefully placed around the sample, the decay positrons are detected and time-stamped. It is possible to calculate the asymmetry in the positron emission as a function of time, $A(t)$, using the collected histograms from the forward (F) and backward (B) detectors, $A(t) = \frac{N_F(t) - \alpha N_B(t)}{N_F(t) + \alpha N_B(t)}$, where α is a calibration factor for the instrument and $N_F(t)$ and $N_B(t)$ are the number of positrons counted in the forward and backward detectors, respectively. Detectors are placed longitudinally during ZF- μSR , and a correction coil is used to cancel out any stray magnetic fields up to 10^{-4} mT. To investigate the time reversal symmetry ZF- μSR measurements were carried out [31]. In the vortex state, TF- μSR measurements were performed with applied fields of 20, 30, 40, 50, and 60 mT, which is greater than the lower critical field H_{c1} (~ 5 mT) and lower than the upper critical field H_{c2} (~ 1 T) [21]. The sample was covered using a thin silver foil after being mounted onto a high purity (99.995%) silver sample holder using diluted GE-varnish. The sample was cool down to 300 mK using a dilution refrigerator. To generate the vortex lattice by trapping the applied TF, we applied field above T_C and then sample was cooled in the field to the base temperature of 300 mK. We used WiMDA [32] software to analyze the μSR data.

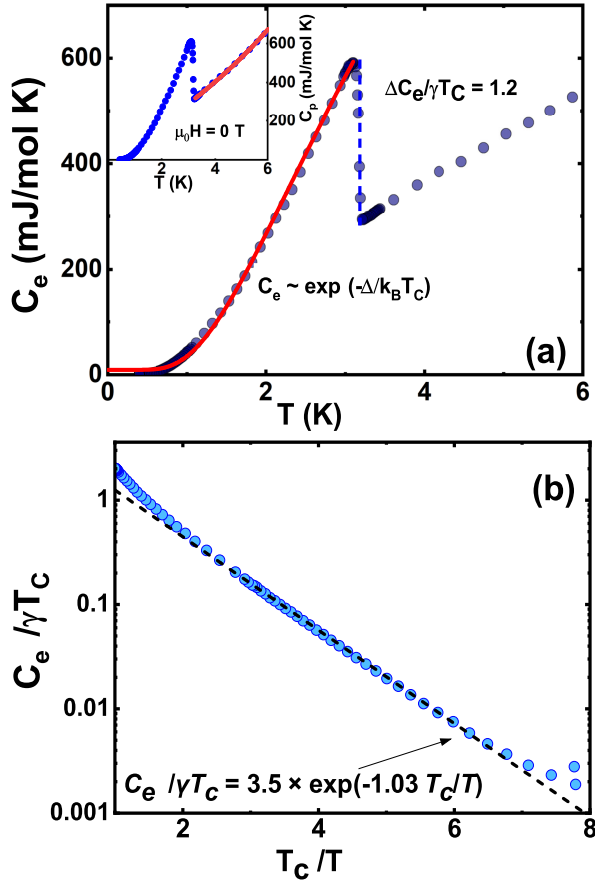


Figure 2. **(a)** Low-temperature specific heat of the filled skutterudite compound $\text{LaOs}_4\text{As}_{12}$, expressed as C_e vs T in a zero magnetic field. The specific heat data is shown in the inset. **(b)** The normalized electronic specific heat ($C_e/\gamma T_C$) versus inverse reduced temperature (T_C/T). The heat capacity data are from [25].

III. RESULTS AND DISCUSSION

A. Crystal Structure & Physical Properties

$\text{LaOs}_4\text{As}_{12}$ crystallizes in a CoAs_3 -type skutterudite structure packed with La atoms and has a body-centered cubic structure with the space group $Im\bar{3}$ (No. 204) as shown in Figure 1. The large icosahedron cage made of As atoms is located around the electropositive La sites, which lack four-fold rotational symmetry. Between the cages, a transition metal ion called Os forms a cubic sublattice. The low temperature specific heat measurements C_P as a function of temperature at zero magnetic field are shown in the inset of Figure 2a. Using the equations $C_P = \gamma T + \beta T^3$, the normal state heat capacity is fitted. We calculated the lattice contribution to the specific heat $\beta = 0.613$ mJ/mol K^4 and the electronic parameter (Sommerfeld's coefficient) $\gamma = 90.47$ mJ/mol K^2 from this. The Debye temperature is determined using the Debye model as $\Theta_D = \left(\frac{12\pi^4 nR}{5\beta}\right)^{1/3}$, where R is the universal gas constant, which is 8.314 J/mol-K, and n denotes the number of atoms in the compound ($n = 17$). The value of Θ_D

is thus calculated to be approximately 377 K, which agrees with the previous measurement [22, 25]. Figure 2a displays the low- T electronic specific heat C_e that was produced after the phonon contribution was taken into account. The heat capacity jump at T_C ($\Delta C_e/\gamma T_C$) is calculated to be 1.2, which is less than 1.43 the value expected for a weak-coupling BCS superconductivity. The fit to the exponential temperature dependency of $C_e(T)$ yields $\Delta(0) = 0.40$ meV, which is close to the 0.45 meV value obtained from the TF- μ SR data analysis (discussed in section-B). Thus, the value of $2\Delta(0)/k_B T_C = 2.9$, which is less than the 3.53 anticipated for weak-coupling BCS superconductors. However, the linear fitting shown in Figure 2b shows that this material exhibits BCS behavior with a single isotropic gap.

B. Superconducting Gap Structure: TF- μ SR

The pairing mechanism and superconducting gap structure of the $\text{LaOs}_4\text{As}_{12}$ were investigated by TF- μ SR experiments down to 0.3 K. The TF- μ SR asymmetry time spectra in the presence of 20 mT and 50 mT applied magnetic fields at above and below T_C are shown in Figures 3a–d. Because of the extra inhomogeneous field distribution of the vortex lattice generated inside the superconducting mixed state of $\text{LaOs}_4\text{As}_{12}$, the spectrum in Figure 3a,c in the superconducting state at 0.3 K demonstrate a greater relaxation. Using the Gaussian damped decay function, the asymmetry spectra were fitted [33–35] using the following equation,

$$A_{\text{TF}}(t) = A_{\text{sc}} \exp\left(-\frac{\sigma_{\text{TF}}^2 t^2}{2}\right) \cos(\gamma_{\mu} B_{\text{sc}} t + \phi) + A_{\text{bg}} \cos(\gamma_{\mu} B_{\text{bg}} t + \phi). \quad (1)$$

The gyromagnetic muon ratio is $\gamma_{\mu}/2\pi = 135.53$ MHz/T, and the initial asymmetries of muons stopping on the sample and on the silver holder are A_{sc} and A_{bg} , respectively (constant across the entire temperature range). The local fields B_{sc} and B_{bg} represent muons stopping on the sample and on the sample holder, respectively, whereas ϕ represents initial phase value and σ_{TF} represents the Gaussian depolarization rate. We calculated the values of $A_{\text{sc}} = 76\%$ and $A_{\text{bg}} = 24\%$ of the total asymmetries by fitting 0.3 K data. When additional temperature data were analyzed, A_{bg} was kept constant and A_{sc} was found nearly temperature independent. The emergence of bulk superconductivity is indicated by an increase in the σ_{TF} rate as the system approaches the superconducting state. With the use of the following formula, the superconducting contribution to the relaxation σ_{sc} was determined, $\sigma_{\text{sc}} = \sqrt{\sigma_{\text{TF}}^2 - \sigma_{\text{nm}}^2}$, where the nuclear magnetic dipolar contribution, is denoted by the symbol σ_{nm} , which is derived from high-temperature fits and is temperature independent. Figure 3e depicts the temperature dependence of σ_{sc} in several applied TF fields. Due to low H_{c2} value, as seen in Figure 3f, σ_{sc} depends on the applied field. Brandt demonstrated that the London penetration depth $\lambda_L(T)$ is linked to σ_{sc} for a super-

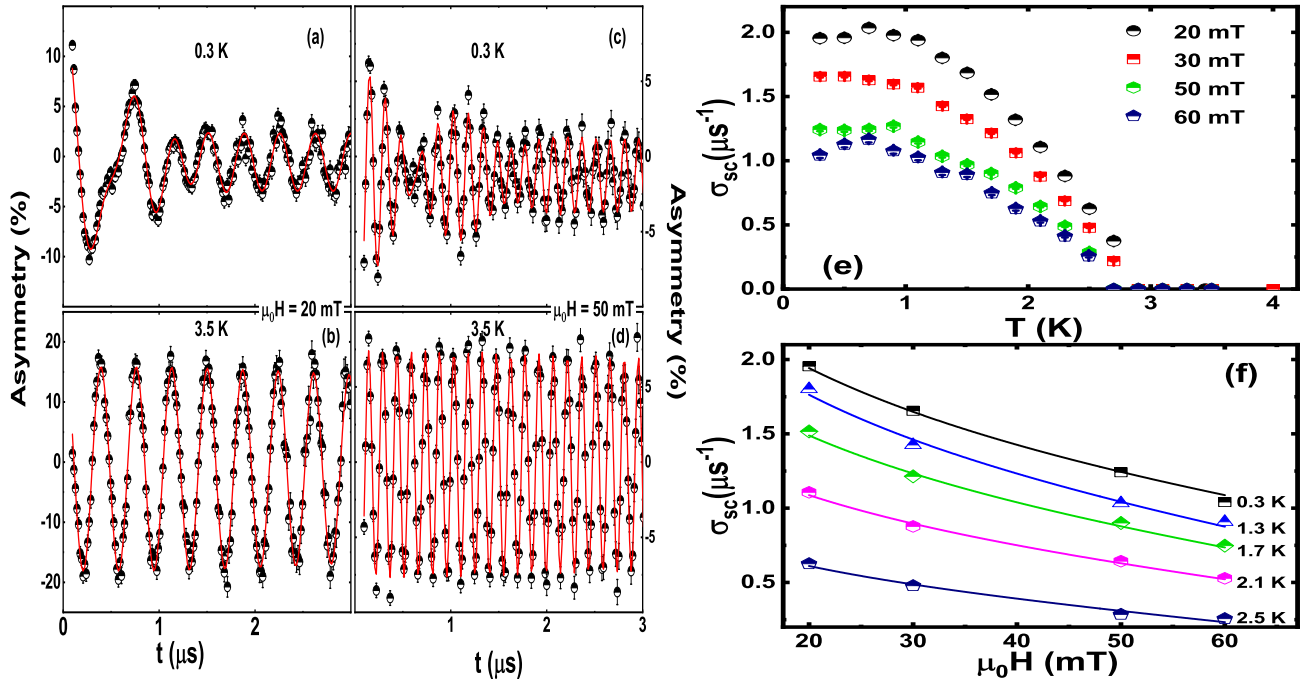


Figure 3. **Left panel:** Asymmetry spectra of the TF- μ SR in the low time region obtained in 20 mT and 50 mT applied magnetic fields at (a–c) $T = 0.3$ K (i.e., below T_C) and (b–d) $T = 3.5$ K (i.e., above T_C). **Right panel:** (e) The superconducting depolarization rate σ_{sc} as a function of temperature in the presence of an applied field of $20 \leq \mu_0 H \leq 60$ mT. (f) The magnetic field dependence of the muon spin depolarization rate is shown for a range of different temperatures. The solid lines are the results of fitting the data using Brandt's equation as discussed in Equation (2).

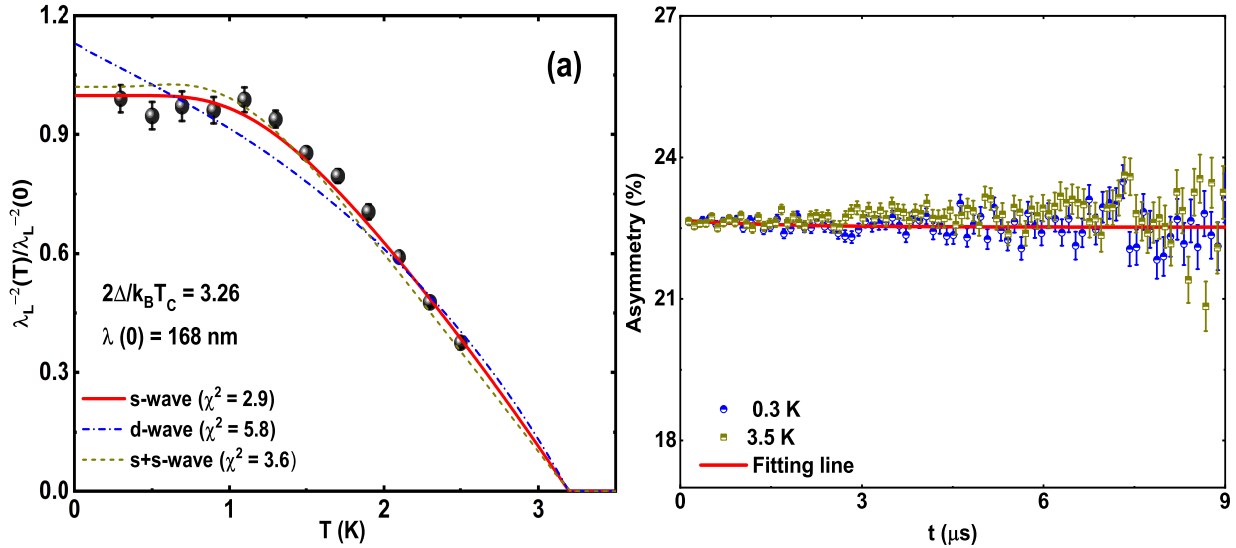


Figure 4. **Left panel :** (a) The inverse magnetic penetration depth squared as a function of temperature is shown here. The lines show the fits using s -wave (red), $s + s$ -wave (light green) and d -wave (blue) gap functions. **Right panel :** (b) Shows the ZF- μ SR spectra for $\text{LaOs}_4\text{As}_{12}$ at 0.3 K (blue) and 4 K (light green). The solid line fits to the experimental data points, as stated in the text.

conductor with $H_{\text{ext}}/H_{c2} \leq 0.25$ [36, 37].

$$\sigma_{sc} [\mu\text{s}^{-1}] = 4.83 \times 10^4 (1 - H_{\text{ext}}/H_{c2}) \times [1 + 1.21 [1 - \sqrt{(H_{\text{ext}}/H_{c2})}]^3] \lambda_L^{-2} [\text{nm}]. \quad (2)$$

This relationship has been used to compute the temperature

dependency of $\lambda_L(T)$. As demonstrated in Figure 3f, isothermal cuts perpendicular to the temperature axis of σ_{sc} data sets were utilized to estimate the H -dependence of the depolarization rate $\sigma_{sc}(H)$. The normalized $\lambda_L^{-2}(T)/\lambda_L^{-2}(0)$ temperature variation, which is directly proportional to superfluid density, is shown in Figure 4a. The data were fitted using the following

equation [38, 39]:

$$\frac{\sigma_{sc}(T)}{\sigma_{sc}(0)} = \frac{\lambda_L^{-2}(T)}{\lambda_L^{-2}(0)} \quad (3)$$

$$= 1 + \frac{1}{\pi} \int_0^{2\pi} \int_{\Delta(T)}^{\infty} \left(\frac{\delta f}{\delta E} \right) \times \frac{EdE d\phi}{\sqrt{E^2 - \Delta(T, \phi)^2}},$$

where $f = [1 + \exp(\frac{E}{k_B T})]^{-1}$ is the Fermi function. We take $\Delta_k(T, \phi) = \Delta(T)g_k(\phi)$, where we assume a temperature dependence that is universal $\Delta(T) = \Delta_0 \tanh[1.82\{1.018(T_C/T - 1)\}^{0.51}]$. The magnitude of the gap at 0 K is Δ_0 , and the function g_k denotes the gap's angular dependence, which is equal to 1 for one isotropic energy gap s , 1 for two isotropic $s + s$ wave energy gap and $\cos(2\phi)$ for d -wave gap, where ϕ is the azimuthal angle along the Fermi surface.

Figure 4a illustrates our comparison of three distinct gap models: employing a single isotropic s -gap wave, a multigap $s + s$ -wave gap, and a nodal d -wave gap. As seen in the figure, the superfluid density saturates at low temperatures, which is a characteristic of the s -wave model with a single gap. An isotropic single-band s -wave model with a gap value of 0.45 meV provides the best representation of the data, with a gap to T_C ratio $2\Delta(0)/k_B T_C = 3.26$, which is less than the BCS weak-coupling limit ($=3.53$). On the other hand, the substantial rise in the χ^2 value puts the d -wave model and $s + s$ -wave (multigap) model inappropriate for this system. A two-gap $s + s$ -wave model of multiband superconductivity has been shown to be compatible with the temperature dependence of magnetic penetration depth of LaRu₄As₁₂. The higher gap to T_C ratio computed in the $s + s$ -wave scenario, $2\Delta_1(0)/k_B T_C = 3.73$, is fairly comparable to the value of 3.53 for BCS superconductor in case of LaRu₄As₁₂ [23]. For LaRu₄As₁₂, 2 K specific phonon modes exhibit modest softening when compared to 20 K, demonstrating that the electron-phonon interactions causing the superconductivity have an audible impact on the vibrational eigenstates [23]. Using McMillan's relation, it is also possible to determine the electron-phonon coupling constant (λ_{e-ph}) [40]:

$$\lambda_{e-ph} = \frac{1.04 + \mu^* \ln(\Theta_D/1.45T_C)}{(1 - 0.62\mu^*) \ln(\Theta_D/1.45T_C) - 1.04}. \quad (4)$$

where μ^* is the repulsive screened Coulomb parameter usually assigned as $\mu^* = 0.13$. The calculated value of the λ_{e-ph} is 0.534. The London model is described as $\lambda_L^2 = m^* c^2 / 4\pi n_s e^2$. It connects the effective mass enhancement $m^* [= (1 + \lambda_{e-ph}) * m_e]$, superconducting carrier density $n_s [= m^* c^2 / 4\pi e^2 \lambda_L(0)^2]$, and London penetration depth. By employing the s -wave model, we determined the London penetration depth of $\lambda_L(0) = 168$ nm. The effective mass enhancement is calculated to be $m^* = 1.53 m_e$, and the superconducting carrier density is predicted to be $n_s = 1.53 \times 10^{27}$ carriers m^{-3} . References [24, 41, 42] include a description of the computations in detail. The calculated values of $\lambda_L(0) = 240$ nm, $n_s = 8.6 \times 10^{27}$ carriers m^{-3} and $m^* = 1.749 m_e$ for

LaRu₄As₁₂ [23]. The fitted parameters for LaOs₄As₁₂ and LaRu₄As₁₂ (for comparison) are shown in Table I. To explain the observed nature of the superconducting gap structures, it is important to comprehend the electronic structures of these compounds, which have been carried [28] and the results suggest that the single-band order parameter in LaOs₄As₁₂ seems to be associated with the hybridized As- p and Os- d electronic character of the Fermi surface. On the other hand, the lack of hybridization for the disjointed Fermi surface of LaRu₄As₁₂, may explain its multiband superconducting nature.

Table I. Fitted parameters for LaOs₄As₁₂ and LaRu₄As₁₂.

Model	$\Delta_i(0)$ (meV)	$2\Delta_i(0)/k_B T_C$	T_C (K)	$\lambda_L(0)$ (nm)
LaOs ₄ As ₁₂ (s -wave)	0.45	3.26	3.2	168
LaRu ₄ As ₁₂ ($s + s$ -wave)	1.656, 0.064	3.73, 0.144	10.3	240

C. Preserved Time Reversal Symmetry: ZF- μ SR

In order to determine if there is a spontaneous magnetic field present in the superconducting ground state, we conducted the ZF- μ SR experiment. Figure 4b shows the time evolution of the asymmetry spectra for $T = 0.3$ K $< T_C$ and $T = 3.5$ K $> T_C$. The ZF- μ SR spectra recorded in the normal and superconducting states show the same relaxations that can be found in overlapping ZF- μ SR spectra, indicating that the superconducting state does not show any spontaneous magnetic field or spin fluctuations. This result suggests that the time-reversal symmetry is preserved in LaOs₄As₁₂ superconducting state. The strong resemblance of the ZF- μ SR spectra (above and below T_C) suggests that the time-reversal symmetry is also retained in the superconducting state of LaRu₄As₁₂. In order to fit the ZF data, a Lorentzian function was used [43],

$$G_{ZF}(t) = A_{sc}(t) \exp(-\lambda_{ZF}t) + A_{bg}, \quad (5)$$

where λ_{ZF} is the electronic relaxation rate, A_{sc} stands for the sample asymmetry, A_{bg} for the constant nondecaying background signal. The red line in Figure 4b indicates the fits to the ZF- μ SR data. The ZF- μ SR asymmetry data fitting parameters are $\lambda_{ZF} = 0.754(4) \mu s^{-1}$ at 0.3 K and $\lambda_{ZF} = 0.744(5) \mu s^{-1}$ at 3.5 K. No conclusive evidence of TRS breaking can be found since the relaxation rate change is within the error bar.

IV. SUMMARY

We employed TF- μ SR to determine the gap symmetry of the superconducting state of LaOs₄As₁₂. An isotropic BCS-type s -wave gap model explains the temperature dependence of the superfluid density. The gap to T_C ratio, which was determined from the s -wave gap fit to the superfluid density,

is 3.26; nonetheless, this is smaller than 3.53 expected for conventional BCS systems. The ZF- μ SR spectra at 0.3 K and 3.5 K are strikingly similar, indicating that the time-reversal symmetry is intact. These results open up the possibility of using the compounds LaRu₄As₁₂ and LaOs₄As₁₂ as special research platforms for investigating filled skutterudites for the interplay between single- and multiband superconducting order parameters in conventional systems.

Acknowledgements

We thank T. Cichorek and J. Juraszek for providing LaOs₄As₁₂ sample and the ascii heat capacity data. We

would like to thank T. Cichorek, P. P. Ferreira, R. Lucrezi, J. Juraszek, C. Heil and L. T. F. Eleno for interesting discussions. AB expresses gratitude to the Science and Engineering Research Board for the CRG Research Grant (CRG/2020/000698 & CRG/2022/008528) and CRS Project Proposal at UGC-DAE CSR (CRS/2021-22/03/549). DTA appreciates the support provided by the Royal Society of London for the Newton Advanced Fellowship between the UK and China, the International Exchange between the UK and Japan, and EPSRC-UK (Grant number EP/W00562X/1). We thanks the ISIS Facility for the beam time, RB1520431 [44].

-
- [1] R. Baumbach and M. Maple, (2010, 1-6), <https://doi.org/10.1016/B978-008043152-9.02235-1>.
- [2] B. Sales, D. Mandrus, and R. K. Williams, *Science* **272**, 1325 (1996).
- [3] V. Keppens, D. Mandrus, B. C. Sales, B. Chakoumakos, P. Dai, R. Coldea, M. Maple, D. Gajewski, E. Freeman, and S. Bennington, *Nature* **395**, 876 (1998).
- [4] E. Bauer, N. Frederick, P.-C. Ho, V. Zapf, and M. Maple, *Physical Review B* **65**, 100506 (2002).
- [5] H. Kotegawa, M. Yogi, Y. Imamura, Y. Kawasaki, G.-q. Zheng, Y. Kitaoka, S. Ohsaki, H. Sugawara, Y. Aoki, and H. Sato, *Physical Review Letters* **90**, 027001 (2003).
- [6] D. Adroja, A. Hillier, J.-G. Park, E. Goremychkin, K. McEwen, N. Takeda, R. Osborn, B. Rainford, and R. Ibberson, *Physical Review B* **72**, 184503 (2005).
- [7] J. Zhang, Y. Chen, L. Jiao, R. Gumenuik, M. Nicklas, Y. Chen, L. Yang, B. Fu, W. Schnelle, H. Rosner, *et al.*, *Physical Review B* **87**, 064502 (2013).
- [8] Y. Kawamura, S. Deminami, L. Salamakha, A. Sidorenko, P. Heinrich, H. Michor, E. Bauer, and C. Sekine, *Physical Review B* **98**, 024513 (2018).
- [9] N. Takeda and M. Ishikawa, *Journal of the Physical Society of Japan* **69**, 868 (2000).
- [10] D. Adroja, J.-G. Park, K. McEwen, N. Takeda, M. Ishikawa, and J.-Y. So, *Physical Review B* **68**, 094425 (2003).
- [11] D. Adroja, J. Park, E. Goremychkin, K. McEwen, N. Takeda, B. Rainford, K. Knight, J. Taylor, J. Park, H. Walker, *et al.*, *Physical Review B* **75**, 014418 (2007).
- [12] R. Baumbach, P. Ho, T. Sayles, M. Maple, R. Wawryk, T. Cichorek, A. Pietraszko, and Z. Henkie, *Proceedings of the National Academy of Sciences* **105**, 17307 (2008).
- [13] A. Shankar, T. Chaki, N. Barman, S. Chatterjee, R. Thapa, and P. Mandal, *Indian Journal of Physics* **93**, 1419 (2019).
- [14] S. Sanada, Y. Aoki, H. Aoki, A. Tsuchiya, D. Kikuchi, H. Sugawara, and H. Sato, *Journal of the Physical Society of Japan* **74**, 246 (2005).
- [15] I. Shirovani, T. Uchiyumi, K. Ohno, C. Sekine, Y. Nakazawa, K. Kanoda, S. Todo, and T. Yagi, *Physical Review B* **56**, 7866 (1997).
- [16] M. Maple, N. Frederick, P.-C. Ho, W. Yuhasz, and T. Yanagisawa, *Journal of Superconductivity and Novel Magnetism* **19**, 299 (2006).
- [17] L. Nordström and D. J. Singh, *Physical Review B* **53**, 1103 (1996).
- [18] G. Meisner, *Physica B + C* **108**, 763 (1981).
- [19] I. Shirovani, T. Adachi, K. Tachi, S. Todo, K. Nozawa, T. Yagi, and M. Kinoshita, *Journal of Physics and Chemistry of Solids* **57**, 211 (1996).
- [20] T. Uchiyumi, I. Shirovani, C. Sekine, S. Todo, T. Yagi, Y. Nakazawa, and K. Kanoda, *Journal of Physics and Chemistry of Solids* **60**, 689 (1999).
- [21] I. Shirovani, K. Ohno, C. Sekine, T. Yagi, T. Kawakami, T. Nakanishi, H. Takahashi, J. Tang, A. Matsushita, and T. Matsumoto, *Physica B: Condensed Matter* **281**, 1021 (2000).
- [22] K. Matsuhira, C. Sekine, M. Wakeshima, Y. Hinatsu, T. Namiki, K. Takeda, I. Shirovani, H. Sugawara, D. Kikuchi, and H. Sato, *Journal of the Physical Society of Japan* **78**, 124601 (2009).
- [23] A. Bhattacharyya, D. Adroja, M. Koza, S. Tsutsui, T. Cichorek, and A. Hillier, *Physical Review B* **106**, 134516 (2022).
- [24] A. Bhattacharyya, K. Panda, D. Adroja, N. Kase, P. Biswas, S. Saha, T. Das, M. Lees, and A. Hillier, *Journal of Physics: Condensed Matter* **32**, 085601 (2019).
- [25] J. Juraszek, Z. Henkie, and T. Cichorek, *Acta Physica Polonica A* **130**, 597 (2016).
- [26] J. Juraszek, R. Wawryk, Z. Henkie, M. Konczykowski, and T. Cichorek, *Physical Review Letters* **124**, 027001 (2020).
- [27] M. Marek Koza, D. Adroja, N. Takeda, Z. Henkie, and T. Cichorek, *Journal of the Physical Society of Japan* **82**, 114607 (2013).
- [28] P. Ferreira, R. Lucrezi, C. Heil, and L. Eleno, unpublished (2023).
- [29] Z. Henkie, M. B. Maple, A. Pietraszko, R. Wawryk, T. Cichorek, R. E. Baumbach, W. M. Yuhasz, and P.-C. Ho, *Journal of the Physical Society of Japan* **77**, 128 (2008).
- [30] S. L. Lee, R. Cywinski, and S. Kilcoyne, *Muon science: Muons in physics, chemistry and materials*, Vol. 51 (CRC press, 1999).
- [31] J. E. Sonier, J. H. Brewer, and R. F. Kiefl, *Reviews of Modern Physics* **72**, 769 (2000).
- [32] F. Pratt, *Physica B: Condensed Matter* **289**, 710 (2000).
- [33] A. Bhattacharyya, D. T. Adroja, M. Smidman, and V. K. Anand, *Science China Physics, Mechanics & Astronomy* **61**, 1 (2018).
- [34] A. Bhattacharyya, D. T. Adroja, K. Panda, S. Saha, T. Das, A. J. S. Machado, O. V. Cigarroa, T. W. Grant, Z. Fisk, A. D. Hillier, and P. Manfrinetti, *Physical Review Letters* **122**,

- 147001 (2019).
- [35] D. T. Adroja, A. Bhattacharyya, Y. J. Sato, M. R. Lees, P. K. Biswas, K. Panda, V. K. Anand, G. B. G. Stenning, A. D. Hillier, and D. Aoki, *Physical Review B* **103**, 104514 (2021).
- [36] E. Brandt, *Journal of Low Temperature Physics* **73**, 355 (1988).
- [37] E. H. Brandt, *Physical Review B* **68**, 054506 (2003).
- [38] R. Prozorov and R. W. Giannetta, *Superconductor Science and Technology* **19**, R41 (2006).
- [39] D. T. Adroja, A. Bhattacharyya, M. Telling, Y. Feng, M. Smidman, B. Pan, J. Zhao, A. D. Hillier, F. L. Pratt, and A. M. Strydom, *Physical Review B* **92**, 134505 (2015).
- [40] W. L. McMillan, *Physical Review* **167**, 331 (1968).
- [41] E. E. M. Chia, M. B. Salamon, H. Sugawara, and H. Sato, *Physical Review B* **69** (2004), 10.1103/PhysRevB.69.180509.
- [42] A. Amato, *Reviews of Modern Physics* **69**, 1119 (1997).
- [43] K. Panda, A. Bhattacharyya, D. T. Adroja, N. Kase, P. K. Biswas, S. Saha, T. Das, M. R. Lees, and A. D. Hillier, *Physical Review B* **99**, 174513 (2019).
- [44] D. Adroja and et al., <https://doi.org/10.5286/ISIS.E.RB1520431> (2016).